ACTA METALLURGICA SLOVACA
2020, VOL. 26, NO. 4, 178-183

RESEARCH PAPER

ANALYSIS OF PLASTIC FORMING PARAMETERS IN AISI 441 STAINLESS STEEL

Orlando Di Pietro[1], Giuseppe Napoli[1], Matteo Gaggiotti[1], Roberto Marini[2], Giulia Stornelli[3], Andrea Di Schino[1]

[1]Engineering Department, University of Perugia, Via G. Duranti 93, 06125, Perugia, Italy

[2]Acciai speciali terni S.p.A., Viale B. Brin, 05100 Terni

[3]University of Rome "Tor Vergata", Department of Industrial Engineering, Via del Politecnico 1, 00133 Rome, Italy

*Correspondence: andrea.dischino@unipg.it, Engineering Department, University of Perugia, Via G. Duranti 93, 06125, Perugia, Italy

Received: 26.08.2020
Accepted: 10.09.2020

ABSTRACT

Plastic deformation is the most common technique adopted to manufacture complex shape pieces in the most efficient way. Even higher requirements need to be faced in the different applications. In order to target such requirement quality and compliance tests are carried out aimed to guarantee that these standards are faced. This often means a waste of material and economic resources. A far as concerns welded stainless steel pipes many criticises affecting the general trend of subsequent machining need to be considered. Such critical issues are more evident in the case of ferritic stainless steel with respect to austenitic ones. Therefore, the study of operating and geometric parameters is fundamental in the production process of ferritic stainless-steel tubes, whose use is mainly for the automotive industry. The possibility to simulate by finite element method (FEM) allows to evaluate the effect of geometric parameters and process constraints on plastic deformation tubes capability, thus allowing to properly fit the plastic deformation process to the target shape as a function of the adopted steel.

Keywords: stainless steel; forming process; mechanical properties

INTRODUCTION

The high mechanical and corrosion resistance [1, 2] allows stainless steels to be used in a wide variety of fields like automotive [3, 5], aeronautical [6-8], food [9, 10], energy [11, 12], sintered [13, 14] and three-dimensional (3D) printing [15, 16]. In automotive industry the forming process allow to produce very complex geometries, [17, 18] and up today several tests are carried out to validate the quality with the subsequent requirement of very high times and costs. This is still of greater importance in aeronautical industry: in the last years, a lot of research papers have been published has been concerning materials for aeronautics [19-21]. Relevant results have been achieved in preparing structural and engine metal alloys with optimized properties [22, 23]. The choice of the material to be adopted strongly depends on the type of component, owing to specific stress conditions, geometric limits, environment, production and maintenance [24, 25]. The strong competition in the industrial aeronautic sector pushes towards the production of aircrafts with reduced operating costs, namely, extended service life, better fuel efficiency, increased payload and flight range. From this perspective, the development of new materials and/or materials with improved characteristics is one of the key factors [26]. As a matter of fact in the aeronautical industry, even a tendency to progressively replace steels by composite is growing, stainless steels are still are commonly used for manufacturing aircraft parts such as landing gears, airframes, turbine components, fasteners, shafts, springs, bolts, propeller cones and axles [27, 28]. A successful solution able to optimize the production process reducing costs and times, is the realization of models that allow to simulate the procedure and confirm the quality of product. The numerical simulation is nowadays an essential tool able to improve the production process in terms of reliability and sustainability; through this method is possible to reduce time to market, cost of developing new components and to have a much more accurate knowledge of processing conditions, like forming [29-32]. The finite element method (FEM) is one of this approach mainly used for the prediction of forming car body parts [33-35], in fact is extremely important guarantee a proper procedure of tube bending and a correct simulation of pipe yielding after bending. During the analysis is also necessary to consider the impact of previous production process which create dispersion in mechanical properties and which show a character no longer deterministic bust stochastic. The plastic deformation of pipes caused by mechanical processing, leads an anisotropic behavior which must be studied by mathematical models; Von Mises and Johnson-Cook [36, 37] criteria for example describe the elastic-plastic behavior of isotropic materials, Hill's criterion instead defines the equations for orthotropic and anisotropic materials [38, 39].

In this paper is used a commercial software package adopting Hill's criterion to study the deformation process of ferritic stainless-steel tubes and the results are compared to those resulting from experimental test.

MATERIAL AND METHODS

The material studied in this paper is an AISI 441 stainless steel (X2CrTiNb18 – EN 1.4509). The chemical analysis of the adopted steel is reported in Table 1.

Table 1 Chemical analysis of AISI 441 (main elements, mass %)

Steel grade	C	Cr	Ni	Mo	Others
AISI 441	0.02	17.5-18.5	-	-	TI+NB=0.55%

Pipes with outer diameter OD ranging from 40 to 60 mm and thickness ranging from 1.0 to 1.8 mm are considered (Table 2).

Table 2 Materials used for simulations with their geometric characteristics

Steel grade	Tube diameter (mm)	Tube thickness (mm)
AISI 441	40; 45; 50; 55; 60	1.0; 1.2; 1.5; 1.8

Steel cold rolled and annealed coils are transformed into tubes. The tube has been then welded adopting laser or high-frequency welding techniques [40, 41]. Examples of welded joints microstructure as achieved in the AISI 441 steel by such techniques are reported in Figure 1.
The tube is then tested based on the UNI EN 69892 (6892-1 e - 2) standard.
Tubes are bended according to a process including the adoption of a mandrel, with an upper pressure die of 750 mm and an offset swiper die of 100 mm.
The maximum steel deformation capacity is reported in a type of diagram named *Formability Limit Curve* (FLC), contained in *Formability Limit Diagram* (FLD); these data are obtained by performing repeated Nakazima tests. The deformation process is studied by drawing a pattern of circles on the sample and is measured by the grid method: the circles distortion creates ellipses by which strains can be measured and on the FLD diagram is possible to identify the deformation state points of the material. This diagram, as shown in the Figure 2, contains the Formability Limit Curve (FLC) showing the maximum capacity of a material to be deformed, calculated by carrying out repeated drawing tests and measuring the ultimate breaking deformation along the two perpendicular directions.
The simulation of bending process on tubes with small diameters is carried out using a software that allows to exploit the Hill 48' yield function [42], taking into account parameters like bending radius, bending angle and rotational speed. The numerical calculations are carried out by means of Altair-HyperWorks™ (2017 version). The FEM model used in such investigation is based on the rigid-plastic variational principle and is reported in detail in [5]. The materials properties needed as input parameter for subsequent modelling include: steel density, Young modulus, Poisson ratio, Lankford value and strain hardening coefficient. Numerical values of such properties as adopted in the following calculations are reported in Table 3.The outputs calculated by the software are mapped to obtain information like internal stress, thinning and deformation; the maximum values observed on the grid will be considered the critical point on the geometry. An example of the obtained maps is reported in Figure 3.

a

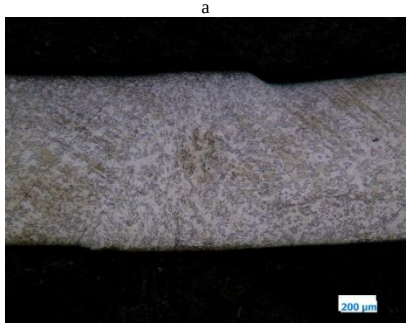

b

Fig. 1 Examples of welded joins in AISI 441 stainless steel tubes. a) laser welded joint, b) high-frequency welded joint

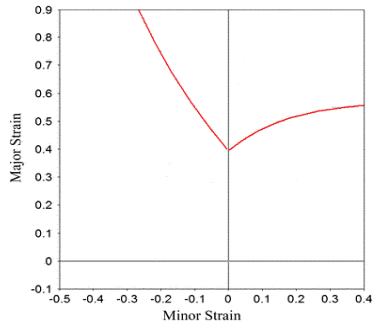

a

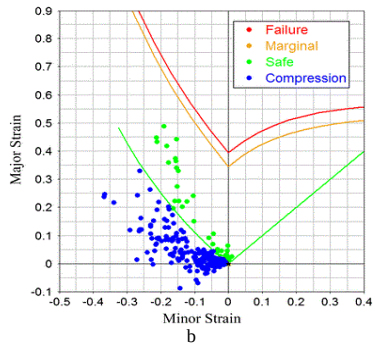

b

Fig. 2 Formability Limit Curve (a); Formability Limit Diagram with deformation state points (b)

Table 3 Steel properties valued adopted in the calculations

Density $\left[\frac{g}{cm^3}\right]$	Young modulus $\left[\frac{N}{mm^2}\right]$	Poisson ratio	Lankford value	Strain hardening
7.8×10^{-9}	210000.0	0.30	1.30–1.40	0.20–0.25

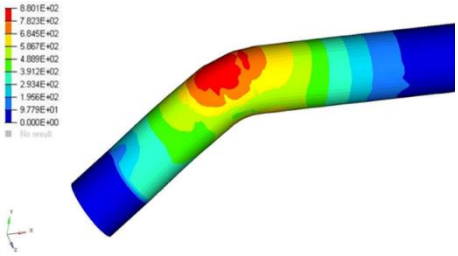

Fig. 3 Stress mapping on tube ben

RESULTS AND DISCUSSION

In the following paragraphs are reported the effects of plastic deformation on the geometry of the tubes.

3.1 Tubes diameter effect

In Figure 4 the stresses behavior as function of the diameters is shown. Results show an effect of approximately 5% of the tubes diameter on the stresses. A similar effect is visible on the tube thinning in Figure 5.

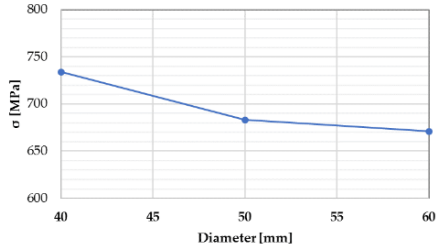

Fig. 4 Mean maximum stress behavior as a function of diameter size for AISI 441 steel - 1.5 mm thickness

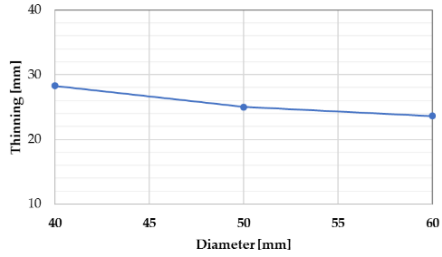

Fig. 5 Maximum thinning as a function of diameter size for AISI 441 steel - 1.5 mm thickness

The results are carried out fixing the ratio between bend radius and diameter R/D at 1.0 value.
The FLD diagrams in Figure 6 reports the behavior of the AISI 441 stainless steel with a diameter sizes ranged between 40 mm and 60 mm; such figure confirms that increasing the diameter decreases considerably the breakage risk.

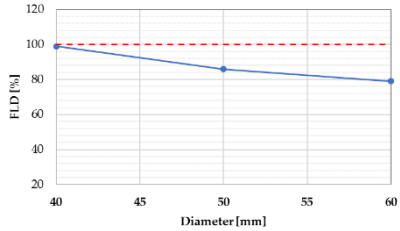

Fig. 6 Formability limit percentage as a function of the tube's diameter for AISI 441 - 1.5 thickness

3.2 Tube thickness effect

The mapping of stresses as a function of thickness is clearly shown in Figure 7, Results report about a not significative stresses distributions (< 2%) when thickness is varied. Different behavior is shown in Figure 8 instead, in which the thinning percentage increases as the tube's thickness increases (variation about 6%).

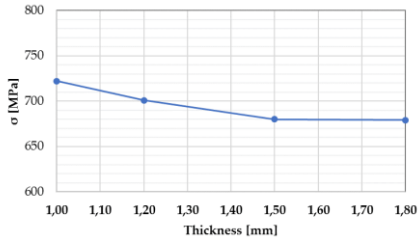

Fig. 7 Mean maximum stress behavior as a function of thickness for AISI 441 steel - 50 mm diameter

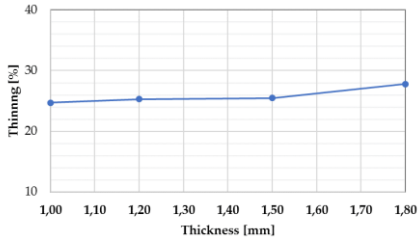

Fig. 8 Maximum thinning as a function of diameter size for AISI 441 steel - 50 mm

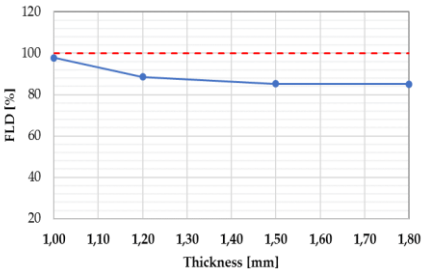

Fig. 9 Formability limit percentage as a function of the thickness for AISI 441 - 50 mm diameter

The FLD plot in function of tube's thickness (Figure 9), shows that an increase of thickness improves the success of bending process.

3.3 Speed rate and bend angle effect

In this section is analyzed the influence of speed variation for bending angle in a common manufacture process range (30° and 90°), in Figure10a and Figure 10b is shown the percentage of formability limit for the combination of angle and thickness. In particular, the geometric parameters were fixed together with the relationship between the diameter and the thickness.

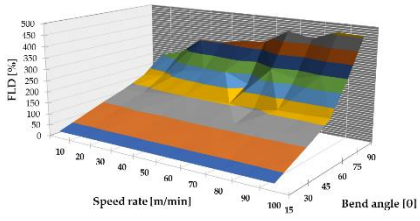

a

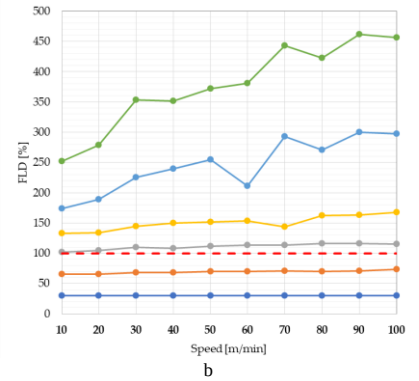

b

Fig. 10 Graph 3D (**a**) and 2D (**b**) of formability limit percentage for each speed and angle combination

Figure 10 reports an interpolation of data shown in Figure 9b, to have a better vision of the speed rate influence. For this reason, the percentage variation between the percentages of formability limits obtained at minimum and maximum feed speed for each angle, calculated according to equation (1), is reported in Figure 12.

$$\Delta FLD = FLDv_{max} - FLDv_{min} \quad (1.)$$

In Figure 12 is possible to see that, in the angle region ranging the 30° and 90° degrees, ΔFLD is related to the slope of interpolated line and this parameter varies almost linearly to the bend angle.
To have a more specified analysis, the study has been repeated using values that fit better the industrial process, the curvature radius was increased, the interpolations were re-performed (Figure 13) and FLD deltas were calculated for the new data obtained.
Figure 14 shows the importance of R/D ratio on the process, the improvement of this parameter in fact leads to an improvement in the sample formability; the ΔFLD increases in the bending angle range 30° - 90° and then tends to be stable away from breaking conditions.

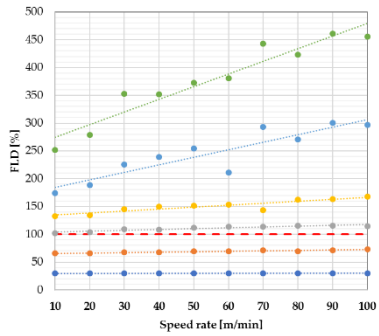

Fig. 11 Linear interpolation of the percentage of the radius of the formability limit for each combination of speed and angle

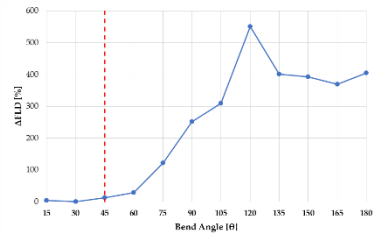

Fig. 12 Goodness of the simulation output beyond the breaking of the worked piece (red dotted line)

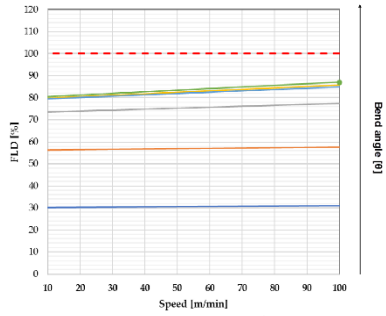

Fig. 13 Improved linear interpolation of the new percentages reached for the formability limit for each combination of speed angle

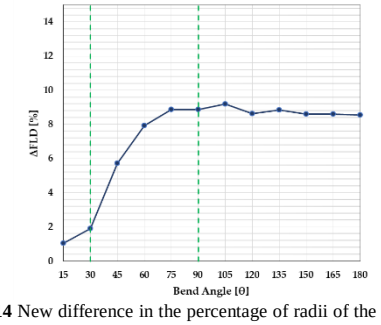

Fig. 14 New difference in the percentage of radii of the formability limit between minimum and maximum speed as a function of the bend angle

3.4 Ratio between bend radius and tube diameter effect

The R/D ratio is a parameter really important in industrial process, in standard conditions the value is between 1.0 and 1.5, in fact for values below 1 the risk of breakage increases. In this case is fixed an R/D = 1 because 1.5 is not used in the automotive field. Performing the simulations with a constant diameter, increasing the bend radius, results show that the stresses do not vary significantly (Figure 15). On the other hand a marked R/D ratio effect is found on the tube's thinning (Figure 16).

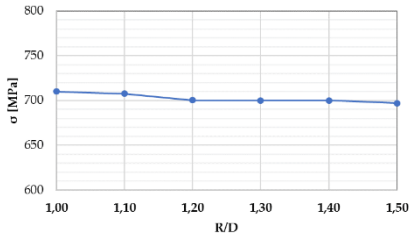

Fig. 15 Maximum equivalent stress dependence on a R/D ratio

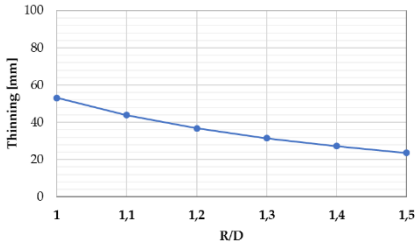

Fig. 16 Maximum equivalent stress dependence on a R/D ratio

CONCLUSION

This paper analyzes the influence of geometric and operational parameters on the bending process of AISI 441 ferritic stainless-steel pipes. It is evaluated an effect of about 5% of tube's diameter on internal stress and the thickness of the tube seems to be a determining factor for the failure and/or undesired deformation of the piece. The variation within the standard industrial operational range (between 1.0 and 1.5) of the R/D ratio, is extremely important because identified the transition between the failure and the success of the operation. Particularly for AISI 441 the variation of this parameter leads to a 60% increase in feasibility. The study of bending angle and speed carried out on the rotational, has shown the tendency to diverge and consequently to have inaccurate results when breaking the piece.

Staying in the non-breaking field instead, allowed to define a trend of influence for these operating parameters, showing how the increase in influence of the rotational speed has a strong impact on the feasibility of the process in the area between 30° and 90° of the angle of fold, while for greater angles there is a stabilization of the results and an effect of variation gradually less.

REFERENCES

1. P. Marshall: *Austenitic Stainless Steels: Microstructure and Mechanical Properties*. Elsevier Applied Science Publisher, Amsterdam, 1984
2. A. Di Schino,Metals, 10, 2020, 327. https://doi.org/10.3390/met10030327
3. W. Liu, J. Lian, J. Munstermann, C. Zeng: Fang, Int. J. of Mech. Sci., 176, 2020, 105534. https://doi.org/10.1016/j.ijmecsci.2020.105534
R. Rufini, O. Di Pietro, A. Di Schino: Metals, 8, 2018, 519. https://doi.org/10.3390/met8070519
4. O. Di Pietro, G. Napoli, M. Gaggiotti, R. Marini, A. Di Schino: Metals, 10, 2020, 1013. https://doi.org/10.3390/met10081013
5. A. Di Schino, L. Alleva, M. Guagnelli: Materials Science Forum, 715-716, 2012, 860. https://doi.org/10.4028/www.scientific.net/MSF.715-716.860
6. A. Di Schino, P.E. Di Nunzio: Acta Metall. Slovaca, 23, 2017, 62. https://doi.org/10.12776/ams.v23i1.852
7. G. Napoli, A. Di Schino, M. Paura, T. Vela: Metalurgija, 57, 2018, 111.
8. A. Di Schino, L. Valentini, J.M. Kenny, Y. Gerbig, I. Ahmed, H. Haefke: Surf. Coat. Technol. 161, 2002, 224. https://doi.org/10.1016/S0257-8972(02)00557-1
9. L. Valentini, A. Di Schino, J.M. Kenny, Y. Gerbig,, H. Haefke: Wear, 253, 2002, 458. https://doi.org/10.1016/S0043-1648(02)00140-0
10. D.K. Sharma, M. Filipponi, A. Di Schino,F. Rossi, J. Castaldi: Metalurgija, 58, 2019, 347.
11. A. Di Schino, C. Testani: Metals 10, 2020, 552. https://doi.org/10.3390/met10040552
12. Z. Brytan, M. Actis Grande, M. Rosso, R. Bidulsky, L.A. Dobrzansky: Materials Science Forum, 627, 2011, 165. https://doi.org/10.4028/www.scientific.net/MSF.672.165
13. R. Bidulsky, M. Actis Grande, E. Dudrova, M. Kabatova, J. Bidulska: Powder Metallurgy, 59, 2016, 121. https://doi.org/10.1179/1743290115Y.0000000022
14. C. Zitelli, P. Folgarait, A. Di Schino: Metals, 9, 2019, 731. https://doi.org/10.3390/met9070731
15. M. Ridolfi, P. Folgarait, A. Di Schino: Materials 13, 2020, 1424. https://doi.org/10.3390/ma13061424
16. K.H. Lo, C.H. She, J.K.L. Lai: Mat. Sci. Eng. R, 65, 2009, 39. https://doi.org/10.1016/j.mser.2009.03.001
17. L. Gardner: Prog. Struct. Eng. Mat., 7, 2005, 45. https://doi.org/10.1002/pse.190
18. F.C. Campbell: *Manufacturing Technology for Aerospace Structural Materials*. Elsevier: Amsterdam, Netherlands, 2006.
19. X. Zhang, Y. Chen, J. Hu: Prog. Aerosp. Sci. 2018, 97, 22. https://doi.org/10.1016/j.paerosci.2018.01.001
20. Z: Huda, P. Edi: Mater. Des. 2013, 46, 552. https://doi.org/10.1016/j.matdes.2012.10.001
21. J. Schijve: *Fatigue of Structures and Materials*. Kluwer Academic Publishers: Dordrecht, Netherlands, 2001.
22. J. J. Cwiek: Achiev. Mater. Manuf. Eng. 43, 2010, 214.
23. W. W Jian et al.: Mater. Res. Lett., 1, 2013, 61. https://doi.org/10.1080/21663831.2013.765927
24. K. Lu. S. Suresh: Science 2009, 324, 349. https://doi.org/10.1126/science.1159610
25. A. Gloria, R. Montanari, M. Richetta, A. Varone: Metals. 9, 2019, 662. https://doi.org/10.3390/met9060662
26. R.L. Klueh, D.S. Gelles, S. Jitsukawa, A. Kimura, G.R. Odette, B. van der Schaaf, M. Victoria,: Nucl. Mater. 2002, 307–311, 455. https://doi.org/10.1016/S0022-3115(02)01082-6
27. M. Wang, Z. Zhou, H. Sun, H. Hu, L. Li: Mater. Sci. Eng. A 2013, 559, 287. https://doi.org/10.1016/j.msea.2012.08.099
28. M.C. Oliveira, J.B. Fernandes: Metals, 9, 2019, 1356. https://doi.org/10.3390/met9121356
29. A .Cherouat, H. Borouchaki, J. Zhang: Metals, 8, 2018, 991. https://doi.org/10.3390/met8120991
30. T. Kvackaj et al.: J. Mater. Eng. Perform., 29, 2020, 1509. https://doi.org/10.1007/s11665-020-04561-y
31. T. Kvackaj et al.: Arch. Metall. Mater., 58, 2013, 407. https://doi.org/10.2478/amm-2013-0008

32. P. Mulidran, M. Siser, J. Slota, E. Spisak, T. Sleziak: Metals, 8, 2018, 435. https://doi.org/10.3390/met8060435
33. M. Mei, G. Khun, Y. He: Chin. J. Aeron., 29, 2016, 305. https://doi.org/10.1016/j.cja.2015.10.011
34. H.J. Bong, F. Barlat,, M. Lee, D.C. Ahn: Int. J. Mech. Sci. 2012, 64, 1. https://doi.org/10.1016/j.ijmecsci.2012.08.009
35. T. Scott, H. Kotadia: Mater. Charact. 163, 2020, 110288. https://doi.org/10.1016/j.matchar.2020.110288
36. S: Wang et al.: Mater. Lett. 2019, 342. https://doi.org/10.1016/j.matdes.2019.108355
37. M. Kaushal, Y.M. Moshi: Soft Matter, 15, 2019, 4915. https://doi.org/10.1039/C9SM00492K
38. O. Cazacu, B. Revil-Baudard, N. Chandola: *Plasticity-Damage Couplings: From Single Crystal to Polycrystalline Materials*. Solid Mechanics and its applications, Vol. 253, Springer International Publishing: Zurich, Switzerland, 2019. https://doi.org/10.1007/978-3-319-92922-4
39. L.D. Frame: Welding Journal, 2012, 34.
40. A. Di Schino, P.E. Di Nunzio, G.L. Turconi: Mater. Sci. Forum, 558-559, 2007, 1435. https://doi.org/10.4028/0-87849-443-x.1435
41. T.B. Yang, Z.Q. Yu, C.B. Xu, S.X. Li: J. Shanghai Jiaotong Univ.,45, 2011, 6.